

Review

Co₃O₄ and Co- Based Spinel Oxides Bifunctional Oxygen Electrodes

M. Hamdani¹, R.N. Singh^{2,*}, P. Chartier³

¹ Laboratoire de Chimie Physique et Pétrologie, Faculté des Sciences, Université Ibn Zohr, B.P. 8106 Cité Dakhla, Agadir Maroc

² Department of Chemistry, Faculty of Science, Banaras Hindu University, Varanasi 221005, India

³ Laboratoire d'Electrochimie et Chimie Physique du Corps Solide, Institut de Chimie LC3-UMR7177 CNRS/UDS, Université de Strasbourg, Strasbourg, France.

*E-mail: rnsbhu@rediffmail.com

Received: 24 December 2009 / Accepted: 15 April 2010 / Published: 30 April 2010

Many spinel cobaltite oxides meet the requirement for a wide range of electrochemical reactions. These materials have largely been investigated as electrocatalysts for the oxygen evolution reaction (OER) or oxygen reduction reaction (ORR). The objective of this article is to summarize the studies available in the literature on electrochemical and electrocatalytic properties of cobaltite spinel oxides towards the OER and ORR in alkaline media. The main focus of this review is on the recent investigations dealing with the performance of Co₃O₄ and Co- based spinel oxides as the oxygen electrodes in the light of the earlier published work.

Keywords: Electrocatalysis; Oxygen evolution; Oxygen reduction; Spinel cobaltites

Contents

1. Introduction
2. Preparation and physico-chemical properties of cobaltite spinel oxides
 - 2.1 Chemical spray pyrolysis technique
 - 2.2 Sol-gel route
 - 2.3 Thermal decomposition method
3. Electrochemical characterization of cobaltites in alkaline media
 - 3.1 Cyclic voltammetry
 - 3.2 Impedance measurement
4. Electrocatalytic properties
 - 4.1 Oxygen evolution reaction
 - 4.2 Oxygen reduction reaction
5. Conclusion

1. INTRODUCTION

The widest class of substances investigated in electrocatalysis is the transition metal oxide systems which have been used for a long time in heterogeneous catalysis. The investigations were focused on dioxides (mainly RuO_2 , IrO_2 , PbO_2 , TiO_2 , SnO_2 ,...), perovskites (mainly LaNiO_3 , LaCoO_3 ,...), pyrochlores ($\text{Pb}_2\text{Ru}_2\text{O}_{7-x}$, $\text{Pb}_2\text{Ir}_2\text{O}_{7-y}$) and spinel-type transition metal oxides ($\text{M}'\text{M}_2\text{O}_4$ with M and M' transition metals, mainly Co_3O_4 and NiCo_2O_4 , ...).

Among spinel type oxides, cobaltites (Co_3O_4 and NiCo_2O_4 spinel oxides), have received great interest, since the seventy of the last century, owing to their use in many industrial applications. These compounds are the most studied ones as oxygen anode and cathode for which promising activity and stability have been demonstrated in alkaline media. In acidic media, these oxide materials are not stable. The advantages of using these oxides as electrode materials are associated with their activity, availability, low cost, thermodynamic stability, low electrical resistance and their environmental friendship. The cationic distribution in the cubic oxide lattice classifies Co_3O_4 as normal and NiCo_2O_4 as inverted spinels [1]. Depending on the valencies of metallic cations, Co_3O_4 and NiCo_2O_4 have long been known to be active and stable catalysts not only for oxygen evolution and reduction, but also for organic electro-oxidation in alkaline media [1-6]. In fact, the presence of mixed valencies of the same cation in such cobaltite spinel systems is helpful for the bifunctional behaviour of the electrodes towards the oxygen evolution reaction (OER) and the oxygen reduction reaction (ORR) by providing donor-acceptor chemisorption sites for the reversible adsorption of oxygen. Also, these oxides exhibit relatively high electrical conductivity by electron transfer taking place with relatively low activation energy between cations of different valencies by hopping processes. The OER is involved as anode reaction in water electrolysis, in metal electrowinning process, etc. Due to the high overpotential of the OER, alkaline water electrolysis normally shows low energy efficiency and efforts have been made to improve the kinetics of the OER to lower the overpotential. On the other hand, the lowering of the overpotential of the ORR is beneficial to the fuel cell development.

The main trend for the electrochemical mechanism of OER or ORR is to involve at least one reaction step with fairly slow electron transfer. For this reason, one of the major aspects to be considered for improving the overall kinetic of the OER or ORR is the nature of the electrode which must be the most efficient and corrosion-resistant. Thus, from an electrocatalytic point of view, the criterion for choosing an appropriate electrocatalyst for practical applications involves a compromise among electrocatalytic activity, thermodynamic stability, corrosion resistance, fabrication cost and long term stability. It is known that electrocatalysis depends on both electronic and geometrical factors. The former ones are those related to the properties that affect the strength of the surface-intermediate bonds and depends on the chemical structure of the surface. The latter factors are those related to the extension of the actual surface area or actual site density and are not directly related to real electrocatalysis since the activation energy of the reaction will not be affected.

Trasatti [7] emphasized that the OER can only proceed when the electrode potential is higher than the potential of the metal/metal oxide couple or the lower metal oxide/higher metal oxide couple. Thus, the ideal couple will be the one which has potential lower or similar to the theoretical potential of the OER. More beneficial effects of the electrocatalysis tend to lowering Tafel slope and increasing

the reaction order. In opposite side, materials with higher overpotentials are suitable for other reactions like O_3 , Cl_2 production and electro-oxidation of pollutants etc. Moreover, Co_3O_4 has also considerable potential for use as electrolytic capacitor [8, 9], as anode in air-metal batteries, and it has also demonstrated high lithium storage capacity and good cycle-ability [10].

$Mn_xCo_{3-x}O_4$ (with $0 \leq x \leq 1$) spinel oxide thin film electrodes, prepared by spray pyrolysis, were studied for peroxide ion production by oxygen reduction reaction for treatment of organic pollutants as encountered in industrial wastes [11, 12]. It is reported that the concentration of HO_2^- (mechanism with 2 electrons) increases when the manganese content increases. In this case, increasing manganese content in this system may orient the reaction of oxygen. The same work reports that, increasing the Mn content catalyzes the ORR and retards the OER. The active centres on which hydrogen peroxides are formed seem to be the Mn^{3+} ions placed in octahedral sites [11]. On the other hand, the surface Co^{3+} ions seem to be the active sites for the OER making Co_3O_4 the most active in the series [13]. $Ni_xCo_{3-x}O_4$ (with $x = 0.3$ and 1) mixed valence oxide nanoparticles/polypyrrole composite electrodes were used to produce H_2O_2 by oxygen reduction in 0.0025M KOH + 0.8M KCl. However, the direct decomposition of the H_2O_2 on the electrode limits its production [14,15].

Recently, the galvanostatic oxidation of cyanide (CN^-) to cyanate (CNO^-), in aqueous base solution has been investigated at a Ti/ Co_3O_4 electrode with reasonable current efficiency [16]. Also, the indirect oxidation of ethylene glycol by peroxide ions resulting from cathodic reduction of O_2 at $Ni_xCo_{3-x}O_4$ spinel oxide thin film electrodes was studied by Chartier and co-workers [17]. The electrochemical activity of these catalyst is correlated to nominal Co^{3+} / Co^{2+} content ratio in the spinel structure and that the more efficient catalyst is $Ni_{0.3}Co_{2.7}O_4$ owing to its highest Co^{3+} / Co^{2+} ratio. Cox and Pletcher [18, 19] have used spinel based electrodes to oxidize alcohol and amine. Due to its higher efficiency, they conclude that the spinel coating may be used for many electrolyses without apparent loss of activity or physical-chemical damage.

Several methods have been used to prepare Co oxide and Co- based spinel oxides. Some of them are thermal decomposition [20-22], spray pyrolysis [23,24], electrostatic spray deposition [25], sol-gel [26-29], precipitation [30-32], electrospinning [33], anodic oxidation of alloys [34], rheological phase reaction and pyrolysis [10], gel hydrothermal oxidation [35], and electrodeposition technique [36-38]. Some of these methods allow obtaining oxides in thin film or in powder forms. Some of these techniques allow spreading the intermediate or the final product on conductive substrates to obtain thin film oxide before the final thermal treatment. The diversification of preparation methods is justified by achieving optimal conditions like low-temperature synthesis, homogeneity of the oxide, controlled morphology, purity of desired phase, stability, high specific surface, inexpensive reagents and good physical and electrochemical properties. The previous parameters are depending on the preparation method, the preparation conditions and the metal salt precursor.

The lattice of Co_3O_4 could host many other metallic cations by partial cobalt substitution.

A survey of the literature reveals that many experimental works have been done on the electroactivity of Co_3O_4 in the last two decades. However, no review article is published according to the best of our knowledge since the work compiled in books edited by Trasatti and others [1-3] in 1980 and 1994. Consequently, the main focus of this article is to review the recent investigations dealing

with the performance of Co_3O_4 and Co- based spinel oxides as the oxygen electrodes in the light of the earlier published work. The results will also be compared with those reported on series of spinel oxides wherever possible.

2. PREPARATION AND PHYSICO-CHEMICAL PROPERTIES OF SOME SPINEL OXIDES

Numerous techniques have been used in the search for the most reliable and cheapest methods for producing Co_3O_4 and cobalt based spinel oxides in thin film or in powder forms. CoFe_2O_4 was prepared by electrodeposition of CoFe_2 alloy films in an ethylene glycol bath followed by an anodization in an aqueous KOH electrolyte to convert them to CoFe_2O_4 . The films have spinel CoFe_2O_4 structure with crystallite size less than 50 nm [39]. A series of ternary ferrite $\text{CoFe}_{2-x}\text{Cr}_x\text{O}_4$ have been synthesized at 70°C by precipitation method and transformed into the film form at the pretreated Ni support using an oxide-slurry painting technique [40].

Despite of the development of many preparation techniques, the three versatile methods, spray pyrolysis technique, sol gel and thermal decomposition would be briefly described in this article. The former allows the preparation of the thin film oxides and the other two methods allow generally the preparation of the powder form oxides.

It is known that the method of preparation of an oxide influences its physicochemical and electrochemical properties. Co_3O_4 is p-type semiconductor and the use of conductive substrate is necessary. Depending on the preparation methods which can involve the oxidation of the substrate (potential, heating,...), an insulating sublayer occurs between the support and the active layer. Trasatti and coworkers [41] made an effort to discriminate between the poor conductivity of the active layer and the insulating barrier at the support/electrocatalyst interface. In the case of Ti/ Co_3O_4 and Ti/ NiCo_2O_4 electrode the authors reported that latter factor is the main cause for uncompensated ohmic losses.

2.1 Chemical spray pyrolysis technique

The chemical spray pyrolysis consists in spraying at room temperature a solution of the reagents, with the help of a vector gas (air, Ar or N_2) on a substrate which is simultaneously heated at a given temperature allowing the decomposition of reagents. The solvent evaporates from the droplets while a chemical process leads to the formation of a solid film on the conductive (metal, ITO,) or non-conductive substrates (glass, quartz,...). This technique, during last three decades, has been one of the major techniques to deposit a wide variety of materials in thin film form, particularly spinel mixed oxides, since Chamberlin and Skarman [42] published in 1966 the first demonstration of spray deposition of a thin solid film on a solid substrate (cadmium sulphide (CdS) films for solar cells). More recently, Patil [23] published an extensive review entitled “versatility of chemical spray pyrolysis technique” where numerous materials prepared by this technique are reviewed. In addition, thin films can be used as electrode for electrocatalysis without adding conducting or binding agents.

Table 1. Preparation conditions and physical parameters of spinel oxide thin films by spray pyrolysis technique.**(a) Co₃O₄**

Oxides	Precursor	Support	P.T. /°C	l / μm	Ω / Ω ⁻¹ cm ⁻¹	a / Å
Co ₃ O ₄ [72]	Co(NO ₃) ₂	G, CdO/G	400–480	<0.5	1.5 ± 1	8.080
Co ₃ O ₄ [78]	Co(NO ₃) ₂	G, quartz, Ti	300-350	≤10	0.016-0.021	8.085
Co ₃ O ₄ [79]	Co(NO ₃) ₂	G, CdO/G, Co	400	1-2	-	8.085
Co ₃ O ₄ [44]	Co(NO ₃) ₂	Co	350	0.4	-	-
Co ₃ O ₄ [16]	Co(NO ₃) ₂	Ti	350	20	-	8.075
Co ₃ O ₄ [44]	Co(NO ₃) ₂	pyrex and glass SnO ₂ : F	150	0.17 -2	-	8.058
Co ₃ O ₄ [5]	Co(NO ₃) ₂	Ti	400	-	-	-
Co ₃ O ₄ [13]	Co(NO ₃) ₂	SnO ₂ /G	420	-	-	8.069
Co ₃ O ₄ [69]	CoCl ₂	G	300	1.9	0.005	8.084

P.T. = Preparation Temp.; l = Thickness; Ω = Conductivity; a = Lattice parameter

(b) Substituted Co₃O₄

Oxides	Precursor	Support	P.T. /°C	l / μm	Ω / Ω ⁻¹ cm ⁻¹	a / Å
NiCo ₂ O ₄ [79]	Co(NO ₃) ₂ , Ni(NO ₃) ₂	G, CdO/G, Co	400	1-2	-	8.115
NiCo ₂ O ₄ [44]	Co(NO ₃) ₂ , Ni(NO ₃) ₂	Co	350	0.5	-	-
NiCo ₂ O ₄ [90]	Co(NO ₃) ₂ , Ni(NO ₃) ₂	Ni	370	-	-	-
NiCo ₂ O ₄ [72]	Co(NO ₃) ₂ , Ni(NO ₃) ₂	G, CdO/G	400-480	2- 4	200	8.112
NiCo ₂ O ₄ [74]	Co(NO ₃) ₂ , Ni(NO ₃) ₂	CdO/pyr-ex glass	400	-	-	-
NiCo ₂ O ₄ [16]	Co(NO ₃) ₂ , Ni(NO ₃) ₂	Ti	350	20	-	8.111
NiCo ₂ O ₄ [78]	Co(NO ₃) ₂ , Ni(NO ₃) ₂	G, quartz, Ti	300-350	≤10	1.5-2.5	8.125-8.129
MnCo ₂ O ₄ [13]	Co(NO ₃) ₂ , Mn(NO ₃) ₂	G/SnO ₂ : F	420	-	-	8.199
Mn _x Co _{3-x} O ₄ [43,44]	Mn(NO ₃) ₂ , Co (NO ₃) ₂	G/SnO ₂ : F	150	-	-	8.058-8.183
Cu Co ₂ O ₄ [53]	Co(NO ₃) ₂ , Cu(NO ₃) ₂	SnO ₂ /G	340	-	33	8.075-8.135

P.T. = Preparation Temp.; l = Thickness; Ω = Conductivity; a = Lattice parameter

Using spray pyrolysis, series of pure Mn_xCo_{3-x}O₄ (0 ≤ x ≤ 1) oxides were synthesized at low temperatures (150°C) onto a glass substrate with a sublayer of SnO₂ by Gautier and co-workers [43, 44]. The physicochemical properties were examined by X-ray and photoelectron spectroscopy. At a

higher temperature (300°C), Patil et al. [45] obtained thin films of pure Co_3O_4 onto amorphous glass substrates. On the other hand, Gautier et al. [46] prepared pure CuCo_2O_4 films at 340°C on conducting glass and studied their electrochemical stability by ex situ spectroscopic analysis. A series of spinel oxides Co_3O_4 , ZnCo_2O_4 , MnCo_2O_4 , FeCo_2O_4 , CuCo_2O_4 and NiCo_2O_4 were synthesized on cobalt substrate and characterized by reflectance spectroscopy [47]. This technique was also used to prepare thin films of Co_3O_4 onto Ni at 300°C [48], LaNiO_3 onto platinum at 500°C [49] and of $\text{Cu}_{1.4}\text{Mn}_{1.6}\text{O}_4$ on non-conducting and conducting glasses and Ni-foils at 530°C [50]. Recently, Hamdani and coworkers have also synthesized thin films of Co_3O_4 on Ti [51], Li- Co_3O_4 on glass [24], and $\text{Ni}_x\text{Co}_{3-x}\text{O}_4$ ($0 \leq x \leq 1$) on Ti [52] for electrocatalysis of OER. As the preparation conditions used in spray pyrolysis are widely different, the physical parameters of thin films of spinel oxides varied much as shown in Table 1.

2.2 Sol-gel route

Originally, sol-gel process used the metal alkoxides as the reagents in organic media to obtain oxides. This technique [53-55] considered as a soft chemistry method, have been used to produce highly porous and large surface oxide powders at relatively low temperatures. It has been found much more advantageous over the solid state synthesis. This technique allows producing nanosized oxide powders. Despite high prices of organometallic precursors, sol-gel-derivative methods are frequently used. Inorganic or organo-inorganic reagents are used in organic or aqueous media. For instance, the latter type of process was used to prepare Co_3O_4 and NiCo_2O_4 . Cobalt salt precursor is dissolved in an organic solvent (propionic acid, maleic acid) [27, 56] to obtain a gel. The following step consists in heating the latter compound at the appropriate temperature in a desired atmosphere. The gel, so obtained, can also be spread out on the conductive substrate followed by thermal treatment [54]. Trasatti et al. [54] prepared a more porous and less crystalline Co_3O_4 by sol-gel route, with the surface concentration of active sites about twice compared with the same oxide prepared by thermal decomposition of nitrate. The crystalline size and the crystallinity of the prepared oxide depend on the oxide composition and drying condition [26]. El Baydi et al [56] reported the relatively higher electrical conductivity for Co_3O_4 by sol-gel method compared with those prepared by nitrate decomposition at the same temperature. Nanosized Co_3O_4 electrodes were prepared using this technique at 400°C by painting titanium support with a mixture of cobalt oxide powder with Teflon and water [57, 58]. Co_3O_4 and CuCo_2O_4 were synthesized by sol-gel method [59]. Co_3O_4 catalyst is granular with an average grain size between 0.5 and 5 μm . However, some authors argued that the fine and small particles produced by sol-gel route may be mechanically unstable [54].

Pure $\text{Cu}_x\text{Co}_{3-x}\text{O}_4$ ($x = 0$ and 1) electrodes were also synthesized by sol-gel method with the BET surface area of 38 and 16 $\text{m}^2 \text{g}^{-1}$ for $x = 0$ and $x = 1$, respectively [60]. Nickel-aluminium-manganese spinel, $\text{Ni}_x\text{Al}_{1-x}\text{Mn}_2\text{O}_4$, were prepared at 350°C and studied in the form of pellets with a maximum activity toward the OER for NiMn_2O_4 [61]. A series of $\text{M}_x\text{Co}_{3-x}\text{O}_4$ ($\text{M} = \text{Cu}, \text{Ni}, \text{or Mn}$) were prepared using a new sol-gel route, wherein the mixed binary solution of chloride of metals, taken as

per stoichiometric requirement of a particular oxide catalyst, was gelified by slow addition of 1M n-butyl amine under stirred condition to pH 10.5 [62].

2.3 Thermal decomposition method

The thermal decomposition of metallic salts is the other technique frequently used to form the oxides in powder form. Also, oxides in thin film forms are prepared by coating the solution of metallic (pure or mixed) salt(s) on a conductive support, drying and subsequent thermal decomposition at a suitable temperature (solution coating method) [53]. The oxides were also prepared by a hydroxide preparation method [40]. In this, an aqueous solution of pure or mixed metal salt(s) treated with an alkali under stirred condition so as to precipitate metal as metal hydroxide. The precipitate, thus obtained, is then transformed into the desired oxide by thermal decomposition at suitable temperatures.

Porous NiCo_2O_4 oxide electrodes were prepared by thermal decomposition at 400°C and compared to NiCo_2O_4 oxide which was prepared by cathodic electrodeposition. The area of the surface active layer of the former is a factor close to 2 higher than those calculated for the latter [53]. Hu et al [63] prepared the binary Ni-Co oxides by thermal decomposition. Co_3O_4 was the major species formed on the electrode when Ni concentration was below 20 m%. When Ni was between 20 and 70/60 m%, NiCo_2O_4 was the major active species and when Ni was above 80 m%, anhydrous NiO with a passive property, was the major species. On the other hand, NiCo_2O_4 was prepared by this technique using metal salts with reproducible results [64]. The study have shown that the preparation parameters such as decomposition temperature, duration of the heat treatment and the catalyst loading determine the morphology of the oxide layer and so influence the performance of the catalyst. ZnCo_2O_4 spinel oxides with particles size of $1.9 \mu\text{m}$ were prepared by thermal decomposition of the metal hydroxide precursors at 350°C for 2 h in air [65]. More complex spinel oxides are also prepared like $\text{Li}_{(1-0.5x)}\text{Fe}_{(1.5x+1)}\text{Mn}_{(1-x)}\text{O}_4$ by calcination of oxides in stoichiometric amounts in oxygen atmosphere at 800°C for 24 h and studied for the OER [66]. In addition, Pereira and co-workers [67] checked the influence of partial substitution of Ni or Co by Cu on the electrocatalytic activity of the NiCo_2O_4 spinel oxide by brushing the nitrate solution onto the pre-treated support, followed by heating at 350°C . This procedure was repeated until the desired thickness was achieved. The same group studied the behaviour of ferrite and metal (Co, Ni or Fe) substituted ferrites [67, 68]. Spinel type ternary ferrites with composition $\text{NiFe}_{2-x}\text{Cr}_x\text{O}_4$ (with $0 \leq x \leq 1$) were synthesized by a precipitation method and subsequent sintering at 400°C for 24 h [69]. Their physicochemical and electrocatalytic properties have been investigated.

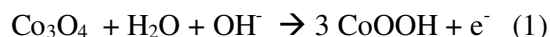
Recently, the combination of microwave and thermal decomposition method yielded to a newly synthesized Co_3O_4 electrode which presents very low overpotential for the OER [70]. Nanosized CoFe_2O_4 oxides were synthesized by the precipitation method following thermal treatment at 380°C [40, 71]. These oxides were used as composite film of polypyrrole and CoFe_2O_4 towards the ORR.

3. ELECTROCHEMICAL CHARACTERIZATION OF COBALTITE OF COBALT IN ALKALINE MEDIA

3.1 Cyclic voltammetry

Co₃O₄

In the late nineties, the cyclic voltammetry study was carried out by two of us [4,72,73] on sprayed Co₃O₄ and NiCo₂O₄ films obtained on CdO/G (G = glass) substrate in 1 M KOH. The rest potentials or the open-circuit potentials for both the oxides were between 0 and 0.05 V vs Hg/HgO in 1M KOH (the potentials are referred to Hg/HgO reference electrode in this text unless otherwise specified). It is reported [16,74] that at the rest potential, the surface of as-deposited oxide film changes partially to the hydrated CoOOH phase as shown in Eq. 1.



The voltammograms of Co₃O₄ present a large potential window from 0.500 to -0.750V. In the positive range of the potential, the fingerprint of Co₃O₄ is characterized by a pair of redox peaks, an anodic at E = 0.520 V (E_{pa}) and a cathodic at E = 0.510 V (E_{pc}), prior to oxygen evolution at the scan rate of 35 mVs⁻¹. These peaks were attributed to the redox couple, CoO₂/CoOOH, which is associated with the formal redox potential (E = (E_{pa} + E_{pc})/2) equal to 0.515 V. The latter remains almost constant, regardless of the potential scan rate. The peak separation potential, ΔE_p (= E_{pa} - E_{pc}), was less than 20mV when the potential scan rate was less than 120 mV/s. The ratio of the anodic peak current, I_{pa}, to the cathodic peak current, I_{pc}, was found close to unity. Taking into account these characteristics, the redox couple behaves like a confined redox couple at the surface of the material.

A value of the formal redox potential, 0.525 V was found with the sprayed Ti/Co₃O₄ films at a slow scan rate [5] in Ar-saturated 1M KOH. Cyclic voltammetric studies on Li-Co₃O₄, prepared by spray pyrolysis technique on glass at 300°C, also showed the typical peaks for the CoO₂/CoOOH redox couple before the onset of oxygen evolution reaction, with the formal redox potential of 0.515 ± 0.005 V, irrespective of amounts of Li incorporated in the oxide lattice [24].

Similar nature of voltammograms on Co-based oxides were later found by others [5, 6, 41, 54, 56, 75-81], irrespective of the preparation procedure and assigned to the formation of a redox couple, CoO₂/CoOOH. The peak prior to the oxygen evolution reported on cobalt oxide deposited at conductive boron-doped diamond [36] was attributed to the establishment of the following redox couple in accordance with other authors [5, 65, 73, 77, 79, 82] too:



Chi et al. [65] also found the establishment of similar redox couple on the catalytic films of the ZnCo₂O₄ on Ni obtained by electrophoretic deposition. This result is in accordance with the thermodynamic redox potentials corresponding to the redox couples, Co₃O₄/CoOOH (E° = 0.222 V vs Hg/HgO) and CoOOH/CoO₂ (E° = 0.562V vs Hg/ HgO) [83, 84].

However, depending on the preparation conditions (technique, temperature, support,...) some difference was noted in the peak potential position of the redox couple involved prior to the commencement of the OER. It is interesting to note that the position and the height of the anodic peak do not change with increasing potential range into the OER region, or polarisation time, indicating that the oxygen formation occurs on an oxidized surface. The voltammogram was stable irrespective of the number of cycle for the same scan rate (v). For $v > 120 \text{ mVs}^{-1}$, the plot of the current peak vs $(v)^{1/2}$ is linear indicating thereby that the surface redox processes are diffusion controlled [73].

The dependence of ΔE_p on the potential scan rate value is more evident for roughened films than that for thin ones, due to variation of the interface resistance induced by the film porosity [78].

The shift of the peaks with scan rate was important and proportional to the roughness. The kinetics of reactions is limited by diffusion process inside the confinement layer. The increase in scan rate invariably shifts the anodic and cathodic peaks. The peaks become farther apart with increasing the scan rate. The anodic and cathodic peak currents increase linearly with increasing the scan rate in the lower scan range and deviate thereafter. So, the surface redox couple can be considered as quasi-reversible one, limited by diffusion controlled process. The standard rate constant, k_s , using Nicholson relation is found to be $10^{-4} \text{ cm s}^{-1}$ [73].

Initially, the same feature of voltammograms was obtained for Co_3O_4 in different concentrations of KOH by Tarasevich and Efrimov [1]. They related this peak to OH^- adsorption as their results showed a shift in the peak potential with the change of pH, i.e. $\partial E_p / \partial \text{pH}$ was about 140 mV/unit pH. A value of $\partial E_p / \partial \text{pH}$ nearly 70 mV/ unit pH was also obtained [5], the ionic strength of the medium being constant.

The shapes of anodic and cathodic peaks change significantly in presence of cyanide ions (CN^-) in solution [16]. The anodic peak becomes larger and the reduction peak progressively decreases. This result indicates that the Co^{4+} species present onto the electrode surface are probably already reduced by direct oxidation of CN^- ions. Further, CV of the $\text{PbO}_2 + \text{Co}_3\text{O}_4$ composite films in 1M NaOH, showed no well defined peak in the potential range preceding the OER [85]. Because of the instability of this oxide in acid solutions, many of the studies were performed in alkaline media. However, an addition of RuO_2 stabilizes Co_3O_4 in sulfuric acid solutions to increase the service time of the electrode when compared to pure oxide and to assess the synergistic effects of the electrode components toward the OER [21, 86, 87]. Another composite oxide, $\text{Ti/RhOx} + \text{Co}_3\text{O}_4$, was prepared and studied in acid solution as function of the composition for supercapacitor applications [9].

In the negative range of the potential, the reduction current starts to increase in deoxygenated 1M KOH below -0.750 V due to the destruction of the oxide lattice [64]. The electrochemical processes may involve the following redox transitions in the negative range of potential.



and



CoO hydrolysed to $\text{Co}(\text{OH})_2$ in alkaline media following :



Consequently in the reverse scan, the potential window diminishes due to appearance of a new large peak A_2 around 0.300 V. The electrochemical oxidation process may be attributed to the redox couple $\text{Co}(\text{III})/\text{Co}(\text{II})$ transition as the height of peak A_1 increased when the voltammogram presents A_2 peak. At this potential, the redox transition involved:



These results were later confirmed by several researchers, namely Palmas et al [58] at Teflon-bonded Co_3O_4 on Ti in 1.75M NaOH, Svegl et al [29], Cassella and Gatta [88], Bocca et al [89] and Trasatti and coworkers [54].

NiCo₂O₄

For sake of comparison, the electrochemical behaviour of NiCo_2O_4 thin oxide films was studied in Ar- saturated KOH 1M [73]. The voltammograms exhibit a single anodic peak, (E_{pa}), and a corresponding cathodic, (E_{pc}), before the oxygen evolution. They, of course, present broader peaks than the ones obtained on Co_3O_4 at less positive potentials. The anodic and the cathodic peak potentials were 0.430 V and 0.370 V, respectively and the ΔE_{p} parameter being, in this case, 60 mV. The $I_{\text{pa}} / I_{\text{pc}}$ ratio was reduced to 0.60. Similar nature of voltammetric curves were reported for sprayed NiCo_2O_4 on Ti ($\Delta E_{\text{p}} = 100$ mV, $E_{\text{p}} = 420$ mV) [5] and on Ni ($\Delta E_{\text{p}} = 170$ mV, $E_{\text{p}} = 405$ mV) [90] in 1M KOH. Similar voltammograms and E_{pa} , E_{pc} and E° values were also reported on Ni/LaNiO₃ films, prepared by spray pyrolysis, in 1 M KOH [91]. However, the anodic and cathodic peaks were relatively sharp due to involvement of only one redox couple, Ni (III) / Ni (II).

It is interesting to note that the position and height of peaks do not change with increasing scanning range into the oxygen evolution region as also noticed with Co_3O_4 oxide films. This indicates that oxygen formation occurs on a completely oxidized surface.

In the case of NiCo_2O_4 , the cathodic polarisation allows the increasing of the bulk reduction current of the oxide around -0.500 V. The lattice destruction occurs relatively easier on NiCo_2O_4 comparatively with Co_3O_4 [72].

3.2. Impedance measurements

The application of electrochemical impedance spectroscopy (EIS) to characterize the electrochemical and electrocatalytic interfacial properties have recently been made in the study of electrocatalysis of oxygen reaction in alkaline solutions. Oxide catalysts are generally obtained in the form of films on conductive supports. Such an oxide catalyst / electrolyte interface can be represented by a simple equivalent circuit model : $\text{LR}_s(\text{R}_1\text{Q}_1) (\text{R}_2\text{Q}_2) (\text{R}_3\text{Q}_3)$, where (R_1Q_1) , (R_2Q_2) , and (R_3Q_3)

correspond to the capacitive and resistive contribution of the catalyst layer / support interface, the bulk catalyst mass, and the electrolyte / catalyst surface, respectively and R_s and L are the solution resistance and inductance, respectively. L is used to include the contribution from the cell connections and their interaction with the surroundings, if any, at high frequencies.

Similar equivalent circuit model have been proposed by Laouini et al [92] for the Co_3O_4 films on the stainless steel support (thermal decomposition method), in 1M KOH. Impedance measurements have been carried out at different positive potentials, from the open circuit potential (OCP) to a potential in the OER region. The roughness factor determined by this proposed model in the potential region, where the charge transfer reaction is negligible, is similar to that obtained by CV. They also obtained Fe (0, 5, 10%) –doped Co_3O_4 [93-94] films on the stainless steel support and determined the impedance spectra in 1M KOH at varying positive potentials with the aim at to characterize the catalyst/solution interface and evaluate the kinetic parameters. In the latter case, $LR_s(R_1Q_1)(R_2Q_2)$ equivalent circuit model was employed to estimate the circuit parameters.

Silva et al. [95] characterized cobalt oxide coatings on cold rolled steel in alkaline sodium sulphate solution by EIS. Coatings were prepared at different temperatures, namely 350, 450, and 550°C. EIS experiments were run at the stabilized open circuit potential, E_{OC} ; and ac signal and frequency range used were 10 mV and 50 kHz to 2 mHz, respectively. The simple equivalent circuit, $R_s(R_{ct}Q_{dl})(R_fQ_f)$, where R_f and Q_f correspond to the resistance and constant phase element for the film, respectively, was employed.

Wu et al. [37] performed impedance measurements on the Co+Ni mixed oxide electrodeposited films on Ni in 1N NaOH at 25°C so as to obtain the mechanistic information in relation to the OER. They proposed the equivalent circuit, $R_s(C_{dl}(R_{ct}(C_pR_p)))$ to model impedance response and estimate the circuit parameters. C_{dl} , R_{ct} , C_p and R_p used in the circuit are the double layer capacitance, charge transfer resistance, pseudo-capacitance and pseudo-resistance, respectively. C_p and R_p are associated with the potential dependent surface coverages of an adsorbed intermediate in the OER mechanism. Similar equivalent circuit, $R_s(C_{dl}(R_{ct}(C_aR_a)))$, was also used by Palmas et al. [96] to model Teflon bonded $\text{Co}_3\text{O}_4/\text{Ti}$ and Nafion bonded $\text{Co}_3\text{O}_4/\text{Ti}$ interfaces in 1N NaOH in the O_2 evolution region ($E = 0.6$ V vs SCE). R_a C_a is a parallel element to take into account for possible adsorption of reaction intermediates. Recently, Singh et al.[69] prepared Co_3O_4 and La doped Co_3O_4 in the form of thin films on Ni and they used the equivalent circuit, $LR_s(R_fQ_f)(R_{ct}C_{dl})$, to treat the impedance data observed in 1M KOH. Palmas et al. [57] investigated the impedance behaviour of $\text{Co}_3\text{O}_4/\text{Ti}$ electrodes in alkaline solution during oxidation runs at different anodic potentials starting from OCP to a potential in the oxygen evolution region (0 to 0.6 V vs SCE) by cyclic voltammetry vis-a-vis impedance spectroscopy. The impedance study was made to better characterize the surface solid state redox transitions (SSRTs). Experimental impedance data were simulated by considering the equivalent circuit model, $R_s(R_1Q_1)(R_2Q_2)$, where R_1 and R_2 and Q_1 and Q_2 represent resistances and pseudocapacitances associated with SSRTs.

Castro et al. [38] obtained mixed anodes of Co and Ni by cathodic electrodeposition on Ni and Fe foils. They also obtained Co + Ni cobaltites by thermal decomposition. The impedance results were analyzed considering a porous electrode and approximated in terms of a finite transmission line model

of conical pores linked in parallel. The impedance analysis carried out and the parameters derived from the fitting procedures allowed successful calculation of the electrochemical active area.

Singh et al. [97, 53] carried out impedance studies on films of $M_xCo_3O_4$ ($M = Cu, Ni$ or Co ; $0 \leq x \leq 1$) obtained on Ni, by precipitation and sol-gel methods, in 1 M KOH at 25°C with the aim to determine the oxide roughness factor. Impedance measurements were carried out in potential region, 0-100 mV, wherein the charge transfer processes were considered to be negligible. The C_{dl} for the oxide / 1M KOH and hence the roughness factor of oxides were determined by both cyclic voltammetry and impedance methods, which were almost similar.

4. ELECTROCATALYTIC PROPERTIES

4.1 Oxygen evolution reaction (OER)

The electrocatalytic activity of Co_3O_4 is studied using the steady-state polarization method, i.e. stationary voltammetry. The potential is incremented from the rest potential to more anodic potential which is sufficient for the OER. Usually, roughness factor (R_f), the Tafel slope (b), the reaction order (p), and some time the exchange current density (i_0), mechanism and thermodynamic data are reported. Depending on the preparation methods and experimental conditions which influence the outcome, the parameters cited above are sometime contradictory.

The roughness factor is defined as the ratio between the determined real surface area and the geometric surface area. Nkeng et al [78] have studied the influence of the addition of alkali nitrate (particularly KNO_3 and $CsNO_3$) in the solution to be sprayed for preparation of Co_3O_4 and $NiCo_2O_4$ oxide films. They found that this addition enhanced the surface area of both the oxide electrocatalysts and yielded oxide films of very high roughness. These films were prepared at 350°C in order to avoid incorporation of alkali ions in the crystallite lattice of spinel.

More recently, Hamdani et al. [24] prepared sprayed thin films of $Li-Co_3O_4$ ($Li/Co = 0, 3, 7,$ and 10%) on Ni at 300°C, followed by the heat treatment at 400°C in air. They observed that Li incorporation into the spinel lattice enlarged the unit cell dimension and increased the electrical conductivity. Values of the lattice parameter (a) and conductivity for the Li-doped oxides were higher than those obtained for un-doped oxide. This increase might result from modification on the cationic distribution in the oxide crystallographic lattice due to the incorporation of Li, or otherwise to particular induced oxide morphology, which favours good contacts between the grains. All the catalytic films demonstrated good potential stability at $i = 50 \text{ mA/cm}^2$ for the OER for more than 40 h. A Tafel slope of 60 mV is quoted for the OER on the prepared films. However, it is reported that introduction of Li in the crystalline lattice of Co_3O_4 has beneficial effect on the activity of the catalyst [24, 98, 99]. In fact, incorporation of Li into the oxide lattice increases the roughness factor, R_f , of Co_3O_4 [24], however, contradictory reports are also available in literature [100]. It is evident from what is stated above that there is no common viewpoint about the influence of incorporation of Li on the roughness factor of Co_3O_4 . On the other hand, in the case of cobaltites, obtained by the hydroxide precipitation method, it is clearly demonstrated that the partial substitution of Ni or Cu for Co in the

Co_3O_4 matrix enhances roughness of the oxide [97]. However, Lal et al. [100] prepared pure and copper-substituted cobaltites by the hydroxide-carbonate-co-precipitation method and investigated in the form of films on nickel for their electrocatalytic properties towards the OER in alkaline solutions. This method for the catalyst preparation markedly improved the roughness as well as the apparent electrocatalytic activity of the oxide compared to one obtained by other methods [4-5, 27, 48, 101]. Moreover, substitution of Co by Cu in the spinel lattice did not indicate any significant influence on the oxide roughness as well as on the rate of the OER.

$\text{M}_x\text{Co}_{3-x}\text{O}_4$ (M = Ni, Cu, Mn) electrodes were also synthesized in films form and investigated their electrocatalytic properties towards oxygen evolution reaction [11, 43, 53, 96]. Hamdani et al. [24] reported that introduction of lithium ion into the Co_3O_4 oxide lattice enhanced the electrocatalytic activity toward the OER. Nikolov et al. [98] also reported the beneficial effects of introduction of Ni, Cu or Li, the effect being the greatest with Li and least with Ni. The activity of Co_3O_4 spinel toward the OER increases with substitution of metal ion in the spinel matrix. Based on activities the oxide electrodes followed the order: $\text{Co}_3\text{O}_4 < \text{Ni}_x\text{Co}_{3-x}\text{O}_4 \leq \text{Cu}_x\text{Co}_{3-x}\text{O}_4 < \text{Li}_x\text{Co}_{3-x}\text{O}_4$. The EOR is considered to take place at Co(IV) sites in the case of pure as well as substituted cobaltites [4, 5, 75].

Table 2. Electrode kinetic parameters for oxygen evolution reaction (OER).

(a) Co_3O_4

Oxides	preparation method	Electrolyte	b / mVdec ⁻¹		p	Ref.
			b ₁	b ₂		
CdO/ Co_3O_4	Spray	1M KOH	60	-	1.3	[4]
Ti/ Co_3O_4	Spray	1-3M KOH	50	-	2	[5]
$\text{SnO}_2\text{:F}/\text{Co}_3\text{O}_4$	Spray	1M KOH	67		1.1	[13]
Ti/Teflon bonded/ Co_3O_4	Sol-gel	1.75M KOH	184	-	-	[58]
CdO/ Co_3O_4	Spray	1M KOH	61-65	-		[78]
Ni/ Co_3O_4	Spray	1M KOH	51-68	120-140	1 or 2	[48]
Pt/ Co_3O_4	Sol-gel	1M KOH	55-60	90-110	-	[29]
Pt/ Co_3O_4	thermal decomposition	1M KOH	60	-	1.7	[101]
Li- Co_3O_4	Slurry method	1M KOH	70	-	-	[115]
Teflon bonded/ Co_3O_4	Freeze-drying	0.4-1.5M KOH	60	120	~ 2	[101]
Ni/Teflonbonded Co_3O_4	Thermal decomposition	15% NaOH at 60°C	145-189	-	-	[32]
Ni/ Co_3O_4	Thermal decomposition	15% NaOH at 60°C	94	140	-	[31]

b = Tafel slope; p = Reaction order

(b) Substituted Co₃O₄

Oxides	preparation method	Electrolyte	b / mVdec ⁻¹		p	Ref.
			b ₁	b ₂		
CdO/NiCo ₂ O ₄	Spray	1M KOH	55	-	1.3	[4]
CdO/NiCo ₂ O ₄	Spray	1M KOH	50-65	-	-	[78]
Teflon bondedNiCo ₂ O ₄	Freeze-drying	5M KOH	46	145		[115]
Teflon bondedNiCo ₂ O ₄	Freeze-drying	1.2-5M KOH	40	120	-	[102]
Ti/NiCo ₂ O ₄	Spray	1-3M KOH	65	-	2	[5]
SnO ₂ :F/MnCo ₂ O ₄	Spray	1M KOH	69	-	1.2	[13]
Cu _{1.4} Mn _{1.6} O ₄	Spray	1M KOH	56-67	-	1.2 & 1.4	[50]
Fe ₃ O ₄	thermal decomposition	1M KOH	63	-		[39]
CuFe ₂ O ₄	thermal decomposition	1M KOH	75	-	-	[39]
CoFe ₂ O ₄	thermal decomposition	1M KOH	42	-	1.86	[105]

b = Tafel slope; p = Reaction order

For the Tafel parameter, usually two Tafel slope values were determined regardless of KOH concentrations. In the case of sprayed CdO/Co₃O₄, the Tafel slope was 60 mV, and the region of linearity extended up to a current value of 0.5 mA/cm² in 1M KOH. This Tafel value indicates that the rate determining step (rds) for the OER on this oxide is the activation controlled process involving one electron transfer [4]. The increase of the Tafel slope in the higher current density region could be due to switch over of the rds from one step to another step. However, there are other factors also which can result a higher Tafel slope at higher potentials / overpotentials; these are mainly the uncompensated IR (ohmic drop) (where R is the sum of contributions of both electrolyte and electrode resistances) and evolving O₂ bubbles on the electrode surface. The latter may block some part of electrochemical active surface area. In 1 M KOH, the Tafel slope values of 61-65 mV and 50 mV were cited respectively at the sprayed CdO/ Co₃O₄ [79] and sprayed Ti/Co₃O₄ [5] electrodes. On the latter electrode, the lowering of the Tafel slope value was observed at higher KOH concentrations, value of slope being 40-45 mV in 3 M KOH.

Table 3. Comparison of the electrocatalytic activity of some spinel oxides toward OER at η= 0.700 V.

Oxides	Technique	Electrolyte	b /mVdec ⁻¹	j / mA cm ⁻²		Ref.
				j _a	j _t	
Co ₃ O ₄	Spray	1M KOH	61-65	0.17-0.86	0.026-0.031	[78]
NiCo ₂ O ₄	Spray	1M KOH	50-65	0.68-9.40	0.08-0.09	[78]
Co ₃ O ₄	Sol-gel	1M KOH	57 & 103	40	0.03	[53]
Ni/ZnCo ₂ O ₄	EPD	1M KOH	70 & 130	161.8-289.6	0.49-0.92	[65]

EPD: Electrophoretique deposition; j_a = apparent current density ; j_t = true current density

Table 4. Comparison of the electrocatalytic activity of some spinel oxides toward OER at $j = 100 \text{ mA cm}^{-2}$

Oxide	Preparation method	Electrolyte	b / mV/dec		η / mV at $j = 100 \text{ mA cm}^{-2}$	Ref.
			b_1	b_2		
NiCo ₂ O ₄	Spray	1M KOH	42	-	457	[90]
Co ₃ O ₄	Sol-gel	1M KOH	75	103	382	[53]
NiCo ₂ O ₄	Sol-gel	1M KOH	52	80	347	[53]
CuCo ₂ O ₄	Sol-gel	1M KOH	65	103	391	[53]
Co ₃ O ₄	T. D.	1M KOH	62	-	398	[97]
NiCo ₂ O ₄	T. D.	1M KOH	53	-	368	[97]
MnCo ₂ O ₄	T. D.	1M KOH	54	-	396	[97]
NiFe ₂ O ₄	T. D.	1M KOH	38	68	352	[69]
NiFeCrO ₄	T. D.	1M KOH	40	60	283	[69]
Fe ₃ O ₄	T. D.	1M KOH	63	-	524	[39]
NiFe ₂ O ₄	T. D.	1M KOH	45	-	431	[39]
CuFe ₂ O ₄	T. D.	1M KOH	75	-	545	[39]
CoFe ₂ O ₄	T. D.	1M KOH	42	89	395	[40]
CoFeCrO ₄	T. D.	1M KOH	43	65	329	[40]

T. D. = Thermal decomposition method

Wu et al. [37] investigated the oxygen evolution kinetics on mixed Co+Ni oxides in alkaline solution by means of the steady state polarization and reported two well defined Tafel slopes, i.e. 40-48 mV at low overpotentials and 110-120 mV at higher overpotentials. Rasiya and Tseung [102] also found two Tafel regions ~40 and ~120 mV respectively at low and higher over potentials.

Spinel oxide films of manganese cobalt with theoretical formula $\text{Mn}_x\text{Co}_{3-x}\text{O}_4$ ($0 \leq x \leq 1$) were prepared by spray pyrolysis at 150°C on conductive $\text{SnO}_2 : \text{F}$ glass [103,13]. XPS analysis reported that Co(III)/Co(II) ratio at the oxide surface decreases with increasing x being equal to 1.2 for Co_3O_4 . The Tafel slopes obtained on the catalytic film series were 67-69 mV [13]. The electrocatalytic activity towards the OER decreases by increasing x . The oxides prepared at 150°C show higher oxygen evolution activity compared to their homologous prepared under the same conditions at 400°C.

Lee, Hu and Wen [104] investigated Co-Cu-Zn ternary oxide system and observed that the introduction of Cu into the oxide lattice enhances the electrocatalytic activity. Singh and coworkers (53) concluded in term of real surface that the order of activities toward the OER is $\text{Ni}_{0.2}\text{Co}_{2.8}\text{O}_4 \approx \text{Ni}_{0.5}\text{Co}_{2.5}\text{O}_4 > \text{Cu}_{0.2}\text{Co}_{2.8}\text{O}_4 > \text{Cu}_{0.5}\text{Co}_{2.5}\text{O}_4 > \text{NiCo}_2\text{O}_4 > \text{CuCo}_2\text{O}_4 \approx \text{Co}_3\text{O}_4$.

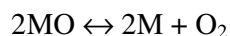
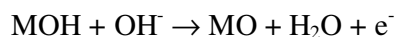
The reaction order with respect to OH^- ion concentration, defined as the slope of plot $\log i$ vs. $\log [\text{OH}^-]$, was found to be very close to 2 with $\text{Ti}/\text{Co}_3\text{O}_4$ in 1M KOH [5]. Other values ranging from 1.0 to 1.2 were also reported [13]. Similar value, i.e. 1.3, is quoted for $\text{CdO}/\text{Co}_3\text{O}_4$ in 1M KOH [4] also. The value of 1.7 was found for $\text{Li-Co}_3\text{O}_4$ in the same electrolyte [24]. Tables 2 to 4 gather some data on electrode kinetic parameters for oxygen evolution reaction.

In few studies related to the oxygen evolution reaction, the thermodynamic data were also determined. Nikolov et al. [48] determined the standard apparent electrochemical activation energy ($\Delta H^{\neq}_{\text{el}}$) of the OER on a number of Co-based oxides at $E = 550 \text{ mV}$ vs Hg/HgO in 3.5 M KOH. The

ΔH°_{el} values were ~76, ~74, ~72, ~75, ~64, ~61, ~45, ~72, and ~64 kJ mol⁻¹ respectively for Co₃O₄, Li_{0.07}Co_{2.93}O₄, Li_{0.22}Co_{2.78}O₄, Cu_{0.2}Co_{3.8}O₄, Cu_{0.5}Co_{2.5}O₄, Cu_{0.7}Co_{2.3}O₄, Cu_{0.9}Co_{2.1}O₄, Ni_{0.2}Co_{2.8}O₄ and NiCo₂O₄. Introduction of Li did not influence ΔH°_{el} for OER on Co₃O₄, while doping of Cu/or Ni reduced it significantly. Spinels were obtained by the thermal decomposition of a mixture of the respective nitrate salts at 350°C for 5h. Singh et al. [97] also found a marked decrease in ΔH°_{el} values with substitution of Cu/or Ni in place of Co in Co₃O₄, obtained by a hydroxide precipitation method; the observed ΔH°_{el} values being ~ 50, ~36, ~39 and ~ 46 kJ mol⁻¹ at E = 0.60 V in 1 M KOH for Co₃O₄, Cu_{0.5}Co_{2.5}O₄, CuCo₂O₄ and NiCo₂O₄, respectively. Similar oxides, namely Co₃O₄, CuCo₂O₄ and NiCo₂O₄, were also obtained by n-butylamine sol-gel precursor route [62] and ΔH°_{el} values for the OER on these oxides respectively were ~52, ~41 and ~47 kJ mol⁻¹. Singh et al [28] also estimated the ΔH°_{el} and ΔS° values on Co₃O₄, obtained by a sol-gel derived route using different metal salt precursors; ΔH°_{el} values ranged between 30 and 48 kJ mol⁻¹ and ΔS° values between -142 and -182 JK⁻¹ mol⁻¹. The ΔH°_{el} and ΔS° values for the OER on La_{1-x}Sr_xCoO₃ (x= 0.1, 0.2, 0.3 and 0.5) and La_{0.7}Sr_{0.3}Co_{0.9}Fe_{0.1}O₃ in 1 M KOH [105] were also determined, ΔH°_{el} values being ~61, ~47, ~49, ~51 and ~60 and ~38 kJ mol⁻¹ with x = 0, x = 0.1, x = 0.2, x = 0.3 and x = 0.5 and Fe = 0.1 mol, respectively; ΔS° values ranged between -133 and -191 J K⁻¹ mol⁻¹. Thus, Sr substitution for La in LaCoO₃ reduced the ΔH°_{el} value. 0.1 mol substitution of Fe in La_{0.7}Sr_{0.3}CoO₃ decreased the ΔH°_{el} further. Similar Sr substituted LaCoO₃ products obtained by stearic acid sol-gel route [106] showed the ΔH°_{el} and ΔS° values ~65 kJ mol⁻¹ and -112 J K⁻¹ mol⁻¹ for x = 0 and ~54 kJ mol⁻¹ and -144 J K⁻¹ mol⁻¹ for x = 0.4. Highly negative ΔS° (standard entropy of activation) values observed for the OER suggest the role of surface adsorption phenomenon in the electrochemical formation of O₂.

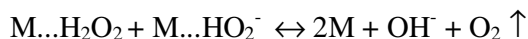
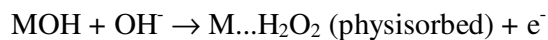
Based on the experimentally observed electrode kinetic parameters (b and p) several mechanisms have been proposed in literature; the important ones were summarized in Table of Ref. [107]. It is observed that most of works reported during recent years have involved mainly three mechanisms to account for the observed Tafel slopes: (i) Bockris's electrochemical oxide path [107], (ii) Bockris and Otagawa's physisorbed-hydrogen peroxide intermediate formation path and [108] (iii) Krasil'shchikov's path [107]. To explain the experimental results, the overall current density expression have been obtained by considering a switch over of the rate determining step (rds) vis-à-vis the adsorption condition during the OER. The outlines of these mechanisms can be given as follows:

Bockris's electrochemical oxide path:

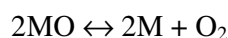
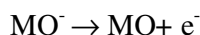
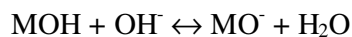


Bockris and Otagawa's physisorbed-hydrogen peroxide intermediate formation path [111]:





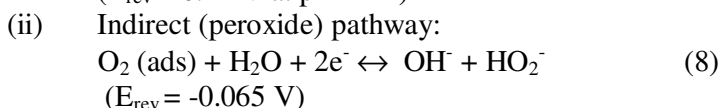
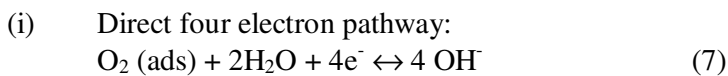
Krasil'shchikov's path:



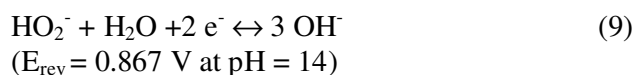
Where, M is an electrochemically active metal ion at the catalyst electrode surface.

4.2 Oxygen reduction reaction (ORR)

Work on oxygen reduction reaction (ORR) on transition metal mixed oxides belonging to perovskite and spinel families of oxides was commenced since after the report by Meadowcroft [109] in 1970 that $\text{La}_{0.8}\text{Sr}_{0.2}\text{CoO}_3$ was a promising electrocatalyst for the ORR in alkaline medium. Before this, Pt was considered as the typical electrocatalyst for the ORR. Among the spinel oxides several Co-based oxides, namely CoCo_2O_4 , NiCo_2O_4 , MnCo_2O_4 , and MgCo_2O_4 were investigated as cathodes for the ORR. Among these, NiCo_2O_4 was the most investigated electrocatalyst. The stationary voltammetry, rotating disk electrode (RDE) and rotating ring disk electrode (RRDE) techniques have been used to study the reaction. Based on results, the following two possible parallel pathways for the ORR were suggested:



Followed by either the further reduction of peroxide ions



Or the catalytic peroxide decomposition



Research work carried out on ORR on cobalt-based oxides up to 1992 have already been comprehensively reviewed [3, 110].

In recent years, Sugawara et al. [111] investigated the ORR on Mn-Co spinel oxides using the RRDE technique. The oxides were prepared by heating the citrate or carbonate precursors at 400 and 600°C in an O₂ atmosphere. A mixture of the oxide and graphite with a weight ratio of 10:90 was kneaded with small amount of paraffin and packed within cavity of gold disk and used as the disk electrode. Among the oxide investigated the oxide with Mn/Co=1.0 and 1.5 were effective oxygen reduction catalysts. Results of the study supported the direct 4-electron reduction of oxygen.

Rios et al. [12] prepared a series of Mn-substituted Co₃O₄ with molecular formulae Mn_{1-x}Co_{3-x}O₄ by the thermal decomposition of the solid residue obtained by evaporation of a mixture of aqueous solutions of mixed metal nitrates in right proportions. Electrodes were in the form of cylindrical pellets which were obtained by mixing the oxide with 85 wt% graphite and a small amount of Teflon under a pressure of 0.5 t cm⁻². The electrodes indicated the Tafel slopes, -60 and -120 mV and the order with respect to OH⁻ concentration, -1. Similar series of spinel oxides were also obtained by Restovic et al. [103] in thin film form on glass and gold substrates using spray pyrolysis technique and studied for the ORR by RRDE technique in 1 M KOH at 25°C. Results showed that the electrocatalytic activity increases when x increases. It was suggested that the cationic distribution that exists in the bulk oxide seems to have a more important influence on the ORR than the distribution on the oxide surface. The Tafel slopes and the order with respect to OH⁻ were the same as already reported in [12].

Rios et al. [11] also studied the ORR on thin sprayed films on Mn_xCo_{3-x}O₄ (0 ≤ x ≤ 1) on Ti in alkaline solutions using the double channel electrode flow cell (DCEFC) with the aim to detect the formation of the intermediate peroxide ions (HO₂⁻). The study showed that the ORR occurs through “interactive” and “parallel” pathways, and the ratio of O₂ molecules reduced to OH⁻ ions with respect to those reduced to HO₂⁻ ions depends on the oxide stoichiometry and on the applied over-potential. The formation of HO₂⁻ ions increases when the manganese concentration increases.

Nissinen et al. [112] obtained nanosized MnCo₂O₄ using a microwave-assisted route of synthesis (MARS) in presence of amorphous carbon and by a conventional method with or without carbon. The study indicated that the catalytic activity of the MARS samples towards ORR in the alkaline electrolyte was more than twice higher than the samples prepared in a conventional oven.

Recently, Koninck et al. [113] found that a partial substitution of 33% Co ions by foreign Co²⁺ ions in Co₃O₄ (i.e. CuCo₂O₄) enhances both the intrinsic O₂ reduction and O₂ evolution [60] activities in 1 M KOH. CuCo₂O₄ favours a total 4e in the O₂ reduction process, based on the rotating ring disk electrode (RRDE). However, the electrode material suffers from the problem of corrosion stability during the cell utilization at higher power density due to the presence of peroxide species (HO₂⁻) in the electrolyte solution. To improve the stability of CuCo₂O₄ at high overpotentials as well as its intrinsic and apparent electrocatalytic activity, they prepared the Mn-doped CuCo₂O₄ (i.e. Mn_xCo_{3-x}O₄) powders and investigated their physicochemical and electrocatalytic properties towards the ORR [114]. The composite film electrodes of the oxides with carbon black Vulcan XC-72R, and poly(vinylidene fluoride-co-hexafluoro-propylene) were obtained on glassy carbon disk surface of a RRDE and studied for ORR in 1M KOH. Results have shown that the manganese content (x value) affects significantly the ORR as well as the intrinsic and apparent electrocatalytic activities. Two different

linear Tafel regions are observed with slopes near -40 and -80 mV dec⁻¹ for low and high overpotentials, respectively, except for Mn_{0.6}Cu_{0.4}Co₂O₄ where only one slope (-41 mV dec⁻¹) is obtained.

5. CONCLUSIONS

The main goal of research work carried out from 1990 to till date (on oxygen evolution/reduction) on Co₃O₄ and substituted products appears to have been to search out a suitable method in order to achieve better homogeneity, controlled morphology, purity of desired phase, high specific surface, stability and good physicochemical and electrocatalytic surface properties. For the purpose, oxides have been prepared by several methods such as thermal decomposition, freeze drying, spray pyrolysis, precipitation, sol gel, electrophoretic, and microwave assisted decomposition. The oxide catalyst powders are transformed in film/layer form on conductive supports to obtain electrodes for investigation. It is noted that almost all the cobaltites, regardless of their preparation methods and of the nature of supports for film preparation, have produced approximately the same values for the Tafel slope, close to $2.303RT/F$ (~60 mV dec⁻¹), for the ORR, however, there is no unanimity in the order for the OER with respect to OH⁻ concentration. Reported values for the order were found to be ~1, ~2 or fractional (between 1 and 2). Most of the research activities related to the ORR seem to be concentrated on manganese substituted Co₃O₄. The electrodes were obtained by mixing the oxide catalyst with graphite, amorphous carbon or carbon black Vulcan XC-72R. Results have demonstrated that the electrocatalytic activity increases with increasing Mn. The RRDE study has established the operation of both the 'direct 4e⁻ pathway' and 'indirect peroxide pathway' mechanisms.

Though, a number of methods have been employed to synthesize the oxide materials, the use of novel methods such as microwave and hydrothermal are scarce; only in one or two reports microwave assisted method have been used and found to be greatly beneficial from electrolysis stand point.

References

1. MR. Tarasevich, BN. Efremov, in: S. Trasatti editor, *Electrodes of conductive metallic oxides, Part A*. Elsevier, Amsterdam (1980), p. 221 and references therein.
2. S. Trasatti, G. Lodi in: S. Trasatti editor, *Electrodes of conductive metallic oxides, Part B*. Elsevier, Amsterdam (1980), p. 521 and references therein.
3. S. Trasatti in: J. Lipkowski, P. N. Ross, editors *Electrochemistry of novel materials*.: VCH publishers Inc., New York (1994), p. 207 and references therein
4. R. N. Singh, M. Hamdani, J. F. Koenig and P. Chartier, *J. Appl. Electrochem.*, 20 (1990) 442.
5. R. N. Singh, J. F. Koenig, G. Poillerat and P. Chartier, *J. Electrochem. Soc.*, 137 (1990) 1408.
6. V. Rashkova, S. Kitova, I. Konstantinov and T. Vitanov, *Electrochim. Acta*, 47 (2002) 1555.
7. S. Trasatti, *Electrochim. Acta*, 36 (1991) 1555.
8. V. Srinivasan and J. W. Weidner, *J. Power Sources*, 108 (2002) 15.
9. A. R. de Sousa, E. Arashiro, H. Golveia and T. A. F. Lassali, *Electrochim. Acta*, 49 (2004) 2051.
10. Z. Yan, F. Huang, C. Feng, Jutang Sun and Y. Zhou, *Materials Chemistry and Physics*, 79 (2003) 1.

11. E. Rios , H. Reyes, J. Ortiz and J. L. Gautier, *Electrochim. Acta*, 50 (2005) 2705.
12. E. Rios , J. L. Gautier, G. Poillerat and P. Chartier, *Electrochim. Acta*, 44 (1998) 1491.
13. E. Rios, P. Chartier and J.L. Gautier, *Solide State Sciences*, 1 (1999) 267.
14. H. Nguyen-Cong, V. de la Garza Guadarrama, J. L. Gautier and P. Chartier, *Electrochim. Acta*, 48 (2003) 2389.
15. H. Nguyen-Cong, V. de la Garza Guadarrama, J.L. Gautier and P. Chartier, *J. New Mater. Electrochem. Systems*, 5 (2002) 35.
16. A. Stavart and A. Van Lierde, *J. Appl. Electrochem.*, 31 (2001) 469.
17. E. Rios, H. Nguyen-Cong, J. F. Marco, J. R. Gancedo, P. Chartier and J. L. Gautier, *Electrochim. Acta*, 45 (2000) 4431.
18. P. Cox and D. Pletcher, *J. Appl. Electrochem.*, 20 (1990) 549.
19. P. Cox and D. Pletcher, *J. Appl. Electrochem.*, 21 (1991) 11.
20. R. Boggio, A. Camgati and S. Trasatti, *J. Appl. Electrochem.*, 17 (1987) 828.
21. L.M. Da Silva, L.A. De Faria and J. F. C. Boodts, *J. Electroanal. Chem.*, 532 (2002) 141.
22. A.C. Tavares, M.A.M. Cartaxo, M.I. da Silva Pereira and F.M. Costa, *J. Solid State Electrochem.*, 5 (2001) 57.
23. P.S. Patil, *Mater. Chem. Phys.*, 59 (1999) 185.
24. M. Hamdani, M.I.S. Pereira, J. Douch, A. Ait Addi, Y. Berghoute and M. H. Mendonca, *Electrochim. Acta*, 49 (2004) 1555.
25. D. P. Lapham, I. Colbeck, J. Schoonman, Y. Kamlag, *Thin solid Films*, 391 (2001) 17.
26. I. Serebrennikova and V. I. Birss, *J. Materials Science*, 36 (2001) 4331.
27. M. El Baydi, S. K. Tiwari, R. N. Singh, J.-L. Rehspringer, P. Chartier, J. F. Koenig and G. Poillerat, *J. Solid State Chem.*, 116 (1995) 157.
28. N. K. Singh, J. P. Singh and R. N. Singh, *Inter. J. Hydrogen Energy*, 27 (2002) 895.
29. F. Svegl, B. Orel, I. Grabec-Svegl and V. Kaucic, *Electrochim. Acta*, 45 (2000) 4359.
30. C. Bo, J.-B. Li, Y.-S. Han and J.-H. Dai, *Materials Letters* 58 (2004) 1415.
31. C. Bocca, A. Barbucci, M. Deluchi and G. Ceriola, *Inter. J. Hydrogen Energy*, 24 (1999) 21.
32. C. Bocca, G. Ceriola, E. Magnone and A. Barbucci, *Inter. J. Hydrogen Energy*, 24 (1999) 699.
33. H. Guan, C. Shao, Y. Liu, N. Yu and X. Yang, *Solid State Communications*, 131 (2004) 107.
34. A. K. M. Fazle Kibria and S. A. Tarafdar, *Inter. J. Hydrogen Energy*, 27 (2002) 879.
35. Y. Jiang, Y. Wu, B. Xie, Y. Xie and Y. Qian, *Mater. Chemistry and Physics*, 74 (2002) 234.
36. N. Sparatu, C. Terashima, K. Tokuhiko and I. Sutanto, *J. Electrochem. Soc.*, 150 (2003) E337.
37. G.Wu, N. Li, D.R. Zhou, K. Mitsuo and B.Q. Xu, *J. Solid State Chemistry*, 177 (2004) 3682.
38. E.B. Castro, S.G. Real and L.F. P. Dick, *Inter. J. Hydrogen Energy*, 29 (2004) 255.
39. S. D. Sartal, V. Ganesan and C. D. Lokhande, *Phys. Stat. Sol.*, 202 (2005) 85.
40. R. N. Singh, N. K. Singh and J. P. Singh, *Electrochim. Acta*, 47 (2002) 3873.
41. D. Baronetto, I. M. Kodintsev and S. Trasatti, *J. Appl. Electrochem.*, 24 (1994) 189.
42. R. R. Chamberlin and J. S. Skarman, *J. Electrochem. Soc.*, 113 (1966) 86.
43. J. L. Gautier, E. Rios, M. Gracia, J. F. Marco and J. R. Gancedo, *Thin Solid Films* 311 (1997) 51.
44. E Rios, G. Poillerat, J.F. Koenig, J.L. Gautier and P. Chartier, *Thin Solid films* 264 (1995) 18.
45. P. S. Patil, L. D. Kadam and C. D. Lokhande, *Thin Solid Films*, 272 (1996) 29.
46. J. L. Gautier, E. Trollund, E. Rios, P. Nkeng and G. Poillerat, *J. Electroanalytical chemistry*, 428 (1997) 47.
47. B. Lefez, P. Nkeng, J. Lopitiaux and G. Poillerat, *Materials Research Bulletin*, 31 (1996) 1263.
48. S. P. Singh, S. Samuel, S. K. Tiwari and R. N. Singh, *Int. J. Hydrogen energy*, 215 (1996) 171.
49. R. N. Singh, L. Bahadur, J. P. Pandey and S. P. Singh, *J. Applied Electrochem.* 24 (1994) 149.
50. A. Restovic, G. PoilLerat, J. F. Koenig and P. Chartier, *Thin Solid Film*, 199 (1991) 139.
51. Ait A. Addi, J. Douch and M. Hamdani, *Bulletin of Electrochem.*, 15 (1999) 556.
52. Ait A. Addi, J. Douch and M. Hamdani, *Annales de Chimie (Paris)*, 23 (1998) 589.

53. R. N. Singh, J. P. Pandey, N. K. Singh, B. Lal. P. Chartier and J.-F. Koenig, *Electrochim. Acta.*, 47 (2000) 1911.
54. G. Spinolo, S. Ardizzone and S. Trasatti, *J. Electroanal. Chem.*, 423 (1997) 49.
55. I. Serebrennikova and V. I. Birss, *J. Electrochem. Soc.*, 147 (2000) 3614.
56. M. El Baydi, G. Poillerat, J.-L. Rehspringer, J. L. Gautier, J.-F. Koenig and P. Chartier, *J. Solid State Chem.*, 109 (1994) 281.
57. S. Palmas, F. Ferrara, A. Vacca, M. Mascia and A.M. Polcaro, *Electrochim. Acta*, 53 (2007) 400.
58. S. Palmas, F. Ferrara, A. Pisu and C. Cannas, *Chem. Papers*, 61 (2007) 77.
59. M. De Koninck, S. C. Poirier and B. Marsan, *J. Electrochem. Soc.*, 153 (2006) A2103.
60. U. Morales, A. Campero and O.Solorza-Feria, *J. New Mater. Electrochem. Systems*, 2 (1999) 89.
61. J. Ponce, J.-L. Rehspringer, G. Poillerat, J. L. Gautier, *Electrochim. Acta*, 46 (2001) 3373.
62. J. P. Singh and R. N. Singh, *Indian J. Chem.*, 39A (2000) 819.
63. C.-C. Hu, Y-S. Lee and T-C. Wen, *Materials Chemistry and physics*, 48 (1997) 246.
64. J. G. D. Haenen, W. Visscher and E. Barendrecht, *J. Applied. Electrochem.*, 15 (1985) 29.
65. B. Chi, J. Li, X. Yang, H. Lin and N. Wang, *Electrochim. Acta*, 50 (2005) 2059.
66. E Rios, Y.-Ychen, M. Gracia, J.F. Marco, J.R.Gancedo and J.L. Gautier, *Electrochim.Acta*, 47 (2001) 559.
67. A. C. Tavares, M. A. M. Cartaxo, M. I. da Silva Pereira and F. M. Costa, *J. Electroanal. chemistry*, 464 (1999) 187.
68. M. Isabel Godinho, M. Alice Catarino, M. I. da Silva Pereira, M. H. Mendonça and F. M. Costa, *Electrochim. Acta*, 47 (2002) 4307.
69. R. N. Singh, J. P. Singh, B. Lal, M. J. K. Thomas and S. Bera, *Electrochim. Acta*, 51 (2006) 5515.
70. R. N. Singh, D. Mishra, Anindita, A. S. K. Sinha and A. Singh, *Electrochem. Comm.*, 9 (2007) 1369.
71. R. N. Singh, B. Lal and M. Malviya, *Electrochim. Acta*, 49 (2004) 4605.
72. M. Hamdani, J. F. Koenig and P. Chartier, *J. Appl. Electrochem.*, 18 (1988) 561.
73. M. Hamdani, J. F. Koenig and P. Chartier, *J. Appl. Electrochem.*, 18 (1988) 568.
74. R. N. Singh, J. F. Koenig, G. Poillerat and P. Chartier, *J. Electroanal. Chem.*, 314 (1991) 241.
75. N. Fradette, and B. Marsan, *J. Electrochem. Soc.*, 145 (1998) 2320.
76. S. Trasatti, Croat., *Chem. Acta*, 63 (1990) 313.
77. M. Longhi and L. Formaro, *J. Electroanal. Chem.*, 464 (1999) 149.
78. P. Nkeng, J.-F. Koenig, J. L. Gautier, P. Chartier and G. Poillerat, *J. Electroanal. Chem.*, 402 (1996) 81.
79. P. Nkeng, G. Poillerat, J.-F. Koenig and P. Chartier, *J. Electrochem. Soc.*, 142 (1995) 1777.
80. R. N. Singh and S. K. Tiwari, *Indian J. Chem.*, 29 (1990) 837.
81. I. Serebrennikova and V. I. Birss, *J. Electroanal.Chem.*, 493 (2000) 108.
82. M. A. M. Cartaxo, T. A. S. Ferreira, M. R. Nunes, M. Helena Mendonça, M. I. da Silva Pereira and F. M. Costa, *Solid State Science*, 9 (2007) 744.
83. E. B. Castro, C. A. Gervasi and J. R. Vilche, *J. Applied Electrochem.*, 28 (1998) 835.
84. M. Pourbaix, *Atlas des équilibres électrochimiques*, Gauthier-Villars.Paris, 1963.
85. M. Musiani, F. Furlanetto and P. Guerriero, *J. Electroanal. Chem.* 440 (1997) 131.
86. L. M. Da Silva, J. F. C. Boodts and L. A. De Faria, *Electrochim.Acta* 45 (2000) 2719.
87. L. M. Da Silva, J. F. C. Boodts and L. A. De Faria, *Electrochim.Acta*, 46 (2001) 1369.
88. I. G. Cassella and M. Gatta, *J. Electroanal. Chem.*, 31 (2002) 534.
89. C. Bocca, A. Barbucci, M. Deluchi and G. Ceriola, *Int. J. Hydrogen Energy.*, 23 (1999) 247.
90. S. K. Tiwari, S. Samuel, R. N. Singh, G. Poillerat, J. F. Koenig and P. Chartier, *Int. J. Hydrogen Energy* 20 (1995) 9.
91. S. P. Singh, R. N. Singh, G. Poillerat and P. Chartier, *Int. J. Hydrogen Energy*, 20 (1995) 203.
92. E. Laouini, M. Hamdani, M. I. S. Pereira, J. Douch, M.H. Mendonca, Y. Berghoute and R. N. Singh, *Int. J. Hydrogen Energy*, 33 (2008) 4936.

93. E. Laouini, M. Hamdani, M. I. S. Pereira, J. Douch, M. H. Mendonça, Y. Berghoute, R. N. Singh, *J. Appl. Electrochem.*, 38 (2008) 1485.
94. E. Laouini, M. Hamdani, M. I. S. Pereira, Y. Berghoute, J. Douch, M. H. Mendonça and R. N. Singh, *Int. J. Electrochem. Sci.*, 4 (2009) 1074.
95. G. C. Silva, C. S. Fugiwara, G. Tremiliosi Filho, P. T. A. Sumodjo and A. V. Benedetti, *Electrochim. Acta*, 47 (2002) 1875.
96. S. Palmas, F. Ferrara, M. Mascia, A. M. Polcaro, J. Rodrigues Ruiz, A. Vacca, G. Piccaluga, *Int. J. Hydrogen Energy*, 34 (2009) 1647.
97. J. P. Singh and R. N. Singh, *J. New Mater. Electrochem Systems*, 3 (2000) 137.
98. I. Nikolov, R. Darkaout, E. Zhecheva, R. Stoyanova, N. Dimitrov and T. Vitamov, *J. Electroanal. Chem.*, 429 (1997) 157.
99. P. Rasiya and A. C. C. Tseung, *J. Electrochem. Soc.*, 130 (1983) 365.
100. B. Lal, N. K. Singh, S. Samuel and R. N. Singh, *J. New Mater. Electrochem. Systems*, 2 (1999) 59.
101. A. Ait Addi, J. Douch and M. Hamdani, *J. Chim. Phy.*, 96 (1999) 1198.
102. P. Rasiya and A. C. C. Tseung, *J. Electrochem. Soc.*, 130 (1983) 2384.
103. A. Restovic, E. Rios, S. Barbato, J. Ortiz and J. L. Gautier, *J. Electroanal. Chem.*, 522 (2002) 141.
104. V. S. Lee, C. C. Hu and T. C. Wen, *J. Electrochem. Soc.*, 143 (1996) 1281.
105. R. N. Singh and B. Lal, *Int. J. Hydrogen energy*, 27 (2002) 45.
106. B. Lal, M. K. Raghunandan, M. Gupta and R.N. Singh, *Int. J Hydrogen Energy*, 309 (2005) 723.
107. John O'M Bockris and T. Otagawa, *J. Phys. Chem.*, 87 (1983) 2960.
108. John O'M Bockris and T. Otagawa, *J. Electrochem. Soc.*, 131 (1984) 209.
109. D. B. Meadowcroft, *Nature*, 226 (1970) 847.
110. E. J. M. O'Sullivan and E. J. Calvo, in "Comprehensive chemical kinetics" R.G. Compton, Editor, Elsevier 1987 p. 304.
111. M. Sugawara, M. Ohno and K. Matsuki, *J. Mater. Chem.*, 7 (1997) 833.
112. T. Nissinen, Y. Kiros, M. Gasik, M. Lampinen, *Material Research Bulletin*, 35 (2004) 1195.
113. M. De Koninck, S.-C. Poirier and B. Marsan, *J. Electrochem. Soc.*, 154 (2007) A381.
114. M. De Koninck and B. Marsan, *Electrochim. Acta*, 53 (2008) 7012.
115. D. B. Hubber, C. R. churchill, *J. Chem. Soc. Faraday Trans.*, 80 (1984) 1965.